

REMARKS

Claim 1 has been amended to include recitations of allowable claim 11 and claim 11 has been canceled.

Claim 12 has been amended to depend from claim 1.

Claim 16 has been rewritten in independent form, and claims 16 and 17 have been amended to make an editorial change.

Claims 1-10 and 12-17 are pending in the application.

The Examiner objects to claim 12 as allegedly having a broader thickness range than set forth in claim 16, from which it depends.

Applicants have amended claim 12 to depend from claim 1 rather than claim 16, since claim 1 does not recite a thickness range. Accordingly, Applicants respectfully request that the Examiner reconsider and withdraw the objection.

The Examiner has objected to claim 11 for allegedly depending from a rejected base claim.

Applicants have amended claim 1 to include recitations of allowable claim 11 and canceled claim 11. Accordingly, based on the amendments, Applicants submit that the objection is moot and claim 1 should be allowable. Therefore, Applicants respectfully request that the Examiner withdraw the objection and allow claim 1.

Claims 1-10, 12 and 14-17 have been rejected under 35 U.S.C. § 103(a) as allegedly being unpatentable over Saitoh et al., U.S. Patent No. 5,612,039 ("Saitoh"), in view of Murray et al., U.S. Patent No. 5,254,662 ("Murray").

Appln. No.: 10/694,839
Amendment under 37 C.F.R. § 1.116

Claim 1 has been rejected under 35 U.S.C. § 103(a) as allegedly being unpatentable over Yanai et al., JP 05-189746 (“Yanai”), view of Murray.

Claim 13 has been rejected under 35 U.S.C. § 103(a) as allegedly being unpatentable over Saitoh as modified by Murray, and further in view of Ushigome, U.S. 5,523,153 (“Ushigome”).

On page 10 of the Final Office Action dated February 23, 2005, the Examiner has indicated that claim 11 contains allowable subject matter. As stated above, Applicants have amended claim 1 to include recitations of claim 11. Accordingly, Applicants submit that claim 1 and claims 12 and 17 depending therefrom, would not be anticipated or obvious over Saitoh or Yanai in view of Murray.

Claim 16 has been rewritten in independent form to include all the recitations of the base claim (claim 1) prior to the above amendment. In this regard, Applicants note that Saitoh teaches that the non-magnetic layer generally has a thickness of 0.5 to 3.0 μm (col. 16, lines 53-56). Applicants’ claims 16 and 17 recite that the thickness range of the conductive layer is 0.02 μm to 0.4 μm (claim 17) or 0.01 μm to 0.4 μm (claim 16). The thickness ranges of the conductive layer in claims 16 and 17 are outside the range disclosed in Saitoh. Further, Saitoh teaches that the non-magnetic layer has a thickness of *preferably* at least 0.8 μm to ensure its advantages (col. 16, lines 53-56), which “teaches away” from the 0.01 to 0.4 μm and 0.02 to 0.4 μm ranges as claimed in claims 16 and 17, respectively. Thus, Applicants submit that the claimed range would not be obvious because Saitoh “teaches away” from such a claimed range.

On page 3 of the Final Office Action dated February 23, 2005, the Examiner acknowledges that Saitoh does not teach the use of a magnetic layer containing CuAu or Cu₃Au type magnetic particles, as required by claim 1. The Examiner uses the teachings of Murray in order to satisfy the deficiency in Saitoh. Therefore, the Examiner concludes that it would have been obvious to one of ordinary skill in the art to substitute the FePt CuAu type particles taught in Murray for the Fe based magnetic particles taught in Saitoh.

In the 1.111 Amendment submitted December 9, 2004, Applicants argued that in order to convert the FePt alloy disclosed in Murray to a ferromagnetic substance usable in a magnetic recording medium of Saitoh, Ushigome, or Yanai, it is necessary to anneal the alloy at a temperature of at least 500 °C after the alloy is coated on the substrate. Applicants argued that the organic substrates of Saitoh, Ushigome, or Yanai could not tolerate the high annealing temperature required to convert the FePt alloy in Murray to a ferromagnetic substance usable in the magnetic recording medium of Saitoh, Ushigome, or Yanai. On page 10 of the Final Office Action dated February 23, 2005, the Examiner asserts that there is no evidence of record to support Applicants' argument. Accordingly, Applicants submit two documents herewith to provide evidential support for this argument.

Saitoh discloses using a PET base in column 21, line 57. Ushigome discloses using a PET base in column 5, line 2. Yanai discloses using a PET film in paragraph [0026] of Yanai.

As described in Table 1 of "Characterization of Magnetic Tapes and Substrates" enclosed herewith, the melting points of PET and PEN are below 300 °C. Additionally, Figs. 7-9 of "Houkouzoku Polyamide Film no Kouzoukaiseki" (Structural analysis of aromatic polyamide

film), Koubunshi Ronbunshu, vol. 51, No. 11 (Nov., 1994) pp. 745-751, enclosed herewith, illustrate that the physical characteristics of an organic film changes below 300 °C. In "Houkouzoku Polyamide Film no Kouzoukaiseki", a PPTA (Paraphenylene terephthal amide) film is used for experiments. In Figs. 7-9, it is clearly shown that crystal characteristics of the film change around 300 °C. In Fig. 8, R(1) refers to the proportion of crystallite size (200) plane of mod. I, and R(2) refers to the proportion of crystallite size (010) plane of mod. II. The crystallinity is $X_c = \sum I_{(hkl)} I_{total} \times 100 (\%)$ in which $I_{(hkl)}$ refers to the intensity for (hkl) plane in an x-ray diffraction. In Fig. 9, H(hkl) refers to the half breadth of the orientation profile of the (010) plane and the (200) plane. Applicants submit that the disclosure in the documents discussed above provides evidence that the organic substrates taught by Saitoh, Ushigome, and Yanai, which have a upper temperature limit of about 400°C, would not withstand the annealing temperature of 500°C required to convert the FePt alloy disclosed in Murray to a ferromagnetic substance useable in a magnetic recording medium. Accordingly, Applicants submit that the presently claimed invention would not be obvious over Saitoh, Ushigome or Yanai in view of Murray because there is no motivation to combine the magnetic medium taught in Saitoh, Ushigome, or Yanai with the magnetic particles taught in Murray and further because the organic substrates disclosed in Saitoh, Ushigome, or Yanai would not work with the magnetic particles disclosed in Murray since the organic substrate of Saitoh, Ushigome, or Yanai cannot tolerate the high annealing temperature required for the magnetic particles of Murray.

Additionally, on page 4 of the Final Office Action dated February 23, 2005, the Examiner asserts that Saitoh meets the recitation “inorganic substrates” because it teaches the use of an organic material filled with an inorganic material (see col. 15, lines 27-30).

Applicants respectfully traverse the rejection for the following reasons. Applicants disagree with the Examiner's comments about the interpretation of the term "inorganic substrate." On pp. 28 to 29 of the specification, Applicants provide examples of the materials that are used as inorganic substrates and organic substrates in the present invention. Since the examples of the materials that are used as inorganic substrates in the specification do not include any material comprising a mixture of an organic material and an inorganic material, it would be apparent to one of ordinary skill in the art reading the specification that the term “inorganic substrate” used in the specification refers to an inorganic support made of an inorganic substance, not a mixture of an organic and inorganic substance. Since the meaning of the term used in the claims should be interpreted in light of the descriptions provided in the specification, the scope of “inorganic substrate” does not include the substrate disclosed in Saitoh.

Accordingly, Applicants submit that claim 16 would not be anticipated or obvious over Saitoh in view of Murray.

In view of the above, Applicants respectfully request that the Examiner reconsider and withdraw the rejections.

Reconsideration and allowance of this application are now believed to be in order, and such actions are hereby solicited. If any points remain in issue which the Examiner feels may be

Appln. No.: 10/694,839
Amendment under 37 C.F.R. § 1.116

best resolved through a personal or telephone interview, the Examiner is kindly requested to contact the undersigned at the telephone number listed below.

The USPTO is directed and authorized to charge all required fees, except for the Issue Fee and the Publication Fee, to Deposit Account No. 19-4880. Please also credit any overpayments to said Deposit Account.

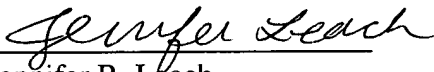
Respectfully submitted,

SUGHRUE MION, PLLC
Telephone: (202) 293-7060
Facsimile: (202) 293-7860

WASHINGTON OFFICE

23373

CUSTOMER NUMBER


Jennifer R. Leach
Registration No. 54,257

Date: April 27, 2005

高分子論文集 (Kobunshi Ronbunshu), Vol. 51, No. 11, pp. 745-751 (Nov., 1994)

芳香族ポリアミドフィルムの構造解析

宮下 憲和^{*}・中尾 辰也^{*}・藤田 忠宏^{*}・藤原 隆^{*}・天野 敏彦^{*}

(受付 1994 年 3 月 28 日・審査終了 1994 年 5 月 11 日)

要 旨 新しい方法で製膜したポリ(パラフェニレンテレフタルアミド) (PPTA) のフィルムの構造形成過程を X 線回折法にて解析した。フィルムは、PPTA の光学異方性濃硫酸液を平板上にキャストし、温度を調節して光学等方性に転移させたのち凝固、乾燥して作成した。乾燥を自由端で行うとフィルムは無配向となり、PPTA の II 型結晶の特徴である (010) 面の反射もほとんど弱れなかった。一方、定長室温乾燥したフィルムでは II 型結晶で (010) 面がフィルム面に平行に積層した面配向構造であった。定長室温乾燥フィルムを高温度で熱処理すると非晶部の結晶化に加えて、II 型結晶の (010) 面配向構造が I 型結晶の (200) 面配向構造に転移した。なお、凝固後の未乾燥湿潤状態ではフィルムは完全に無配向で結晶性も低かった。PPTA フィルムは水凝固させると II 型結晶となることが知られていたが、II 型結晶の配向構造は定長乾燥によって発現することが明らかとなった。

1 はじめに

耐熱性で高強度、高弾性率の高分子材料に対する期待は大きい。剛直な分子鎖を持つ芳香族アミド系高分子は、高強度、高弾性率ポリマー素材として特に注目されてきた。中でもデュボンの開発したポリ(パラフェニレンテレフタルアミド) (以下、PPTA と略記する) 繊維ケブラーは優れた産業素材として有名である。その後、アミド系を初めエステル系、イミド系など多くの芳香族高分子素材の開発、研究がされてきた。PPTA を用いた材料についてもこれまでに多くの報告がなされているが、そのほとんどが繊維に関するものである。PPTA 分子は分子鎖の剛直性からみても耐熱性や機械的物性の優れたフィルム素材であることが期待できるにもかかわらず、フィルムに関する研究はほとんどみられなかった。PPTA の液晶性濃硫酸溶液の流動性は特異であり、高度に一軸配向性である。溶液のこのような流動性は繊維形成には有利であっても、二次元的な配向が要求されるフィルムの成形には極めて不利である。PPTA フィルムに関する研究が少ないのは、フィルム成形技術が確立されていないことが一因と思われる。

PPTA フィルムの成形法に関しては White ら¹⁾の報告がある。彼らは油を塗付したマンドレル上に PPTA ポリ

マー原液を押出し、マンドレル上での原液の流動を制御して分子鎖を面内に配向させ、均質で透明なフィルムを得ている。しかし、この方法はその後実用化されていないようである。また、PPTA フィルムの構造に関しては高柳ら²⁾の優れた報告がある。彼らは実験室で調製した PPTA フィルムを用いて、原液、凝固条件と構造についての詳細な研究を行い、次の重要な知見を得ている。

① PPTA フィルムには I 型と II 型の二つの結晶形が現れる。I 型は繊維にみられる結晶形であり、田所ら³⁾によって解析された。II 型は適当な条件で作成されたフィルムにみられる結晶形で高柳らによって解析された。

② I 型および II 型では (200) 面が水素結合を含む面 (水素結合面と呼ぶ) となっている。I 型結晶は水素結合面がフィルム面と平行に積層した (h00) 面配向を、II 型結晶は、水素結合面がフィルム面に垂直に立った (0k0) 面配向をする。

③ 凝固剤に、メタノール、アセトンなどの有機溶媒を用いた場合、結晶形は I 型を、水を用いた場合には II 型をとる。

④ II 型結晶は熱処理によって I 型に転移する。転移は原液のポリマー濃度による。

我々は、PPTA ドープの相図上の光学異方性-等方性転移を利用して、均質で高度に面配向したバランスフィルムを製膜する工業的プロセスを開発した^{4,5)}。

本報では、このプロセスで生じる PPTA フィルムの結晶化や結晶変態の発生、面配向構造の形成過程について検討した結果を高柳らの結果と対比させつつ報告する。

^{*}1 旭化成工業(株)解析センター (〒882 宮崎県延岡市中川原 5-4960)

^{*}2 旭化成工業(株)MKF プロジェクト (〒882 宮崎県延岡市中川原 5-4960)

^{*}3 武蔵川女子大学家政学部被服学科 (〒663 兵庫県西宮市池田町 6-46)

宮下・中尾・藤田・藤原・天野

2 実 験

2.1 試 料

試料は Fig. 1 に示す流れ図に従って製膜した。光学異方性ドーブ (ポリマー濃度 12 wt%, 固有粘度 $\eta_{inh}=6.5$) をガラス板上にキャストし、温度、湿度を調整して相図上の光学等方性領域に相転移させ、これを水浴中で凝固させて凝潤フィルムを得た。この凝潤フィルムを金属棒に固定し、250°C、2時間乾燥して得られたフィルムを試料1とした。試料1フィルムの厚さは約 20 μm である。また、凝潤フィルムをそのまま自由に収縮できる状態で室温乾燥したフィルムを試料2、金属棒に固定して室温乾燥したフィルムを試料3とした (以後、フィルムの乾燥法として、フィルムを金属棒に固定し乾燥する方法を定長乾燥法と呼び、凝潤フィルムをそのまま自由に収縮できる状態で乾燥する方法を自由端乾燥法と呼ぶ)。試料2、3のフィルム中には約 30 wt% の水分が残存した。なお、熱処理は密閉置換した密閉式電気炉内にフィルムを入れ、所定の温度で1~2分間行った。熱処理温度が 300°C 以上になるとフィルムはゆっくりと茶色に着色し、600°C 以上で炭化した。

2.2 測 定

2.2.1 X線回折測定 X線発生装置として理学電機 (株) 型 RU-200 を、X線として Ni フィルターでろ過した Cu-K α 線を使用した。測定試料として幅 1.0 mm の短冊状に切断したフィルムを方向をそろえて重ね、フィルム製膜方向を Z、フィルム面の法線方向を X、これらに垂直な方向を Y 軸方向とした。回折写真は、測定試料の X, Y, Z 軸方向より X 線を入射させ、平板カメラにて広角 X 線回折写真 (それぞれ X, Y, Z パターンと呼ぶ) を撮った。

回折プロファイルは点焦点を用いた対称透過法によって測定したが、一部、線焦点による反射法測定も行った。得られた赤道上の回折プロファイルは、最小二乗法にて (010), (200), (004) 面の反射および非晶ピークにピーク分離を行った後、(hkl) 面の法線方向への結晶サイズ $S(hkl)$ 、結晶化度 X_c 、および I 型、II 型それぞれの結晶分率 $R(1)$, $R(2)$ を以下の式にて算出した。

[結晶サイズ $S(hkl)$]

Scherrer の式より算出した。

$$S(hkl) = 1 / \cos \theta_{(hkl)} \cdot \sqrt{B_{(hkl)}^2 - B_0^2}$$

ただし

 $\theta_{(hkl)}$ (hkl) 面のブラッグ角 $B_{(hkl)}$ ピーク分離後の (hkl) 面の半値幅 B_0 Si 粉末を利用して求めた光学系の広がり[結晶化度 X_c]

$$X_c = \sum I_{(hkl)} / I_{\text{total}} \times 100 (\%)$$

ただし

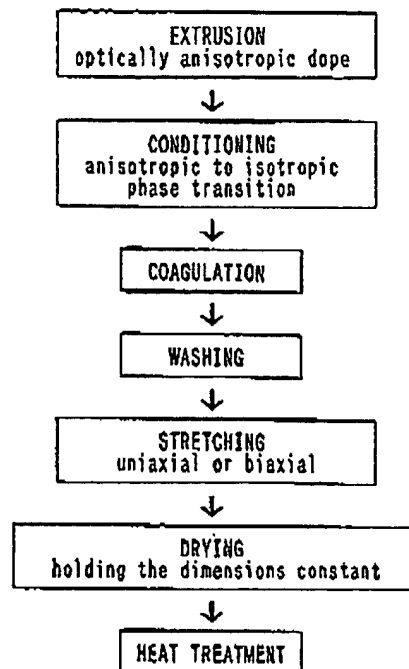


Fig. 1. Block diagram of our manufacturing process of PPTA films.

 $\sum I_{(hkl)}$ (010), (200), (004) 面の積分強度の和 I_{total} 回折プロファイル全体の積分強度[I 型, II 型の結晶分率 $R(1)$, $R(2)$]

$$R(1) = I_{(010)} / I_{\text{total}} \times 100 (\%)$$

$$R(2) = I_{(200)} / I_{\text{total}} \times 100 (\%)$$

ただし

 $I_{(hkl)}$ (hkl) 面の積分強度[配向の目安 $H(hkl)$]

繊維試料台を用いて、II 型の (010) 面と I 型の (200) 面の配向プロファイルを求め、その半値幅 (deg.) を配向の目安 $H(hkl)$ とした。

2.2.2 熱測定 示差走査熱量計 (Perkin Elmer 社製 DSC-IIIC) を用いて、5 mm × 5 mm の小片フィルムを窒素雰囲気下、昇温速度 10°C/min で 30°C から 510°C までを測定した。

3. 結果と考察

3.1 フィルム構造

PPTA の I 型結晶では結晶の対称性によって (010) 面の反射は消滅する²⁾。したがって、観測される (010) 面の反射は II 型結晶によるとみてよい。Fig. 1 の流れ図に沿って製膜した試料1フィルムの X 線回折写真 (Fig. 2(d)) には明らかに (010) 面の反射が観測され、I 型結晶の他に微量の II 型結晶が混在した¹⁰⁾。また、フィルムは高度に面配向しており、I 型結晶はいわゆる (200)

芳香族ポリアミドフィルムの構造解析

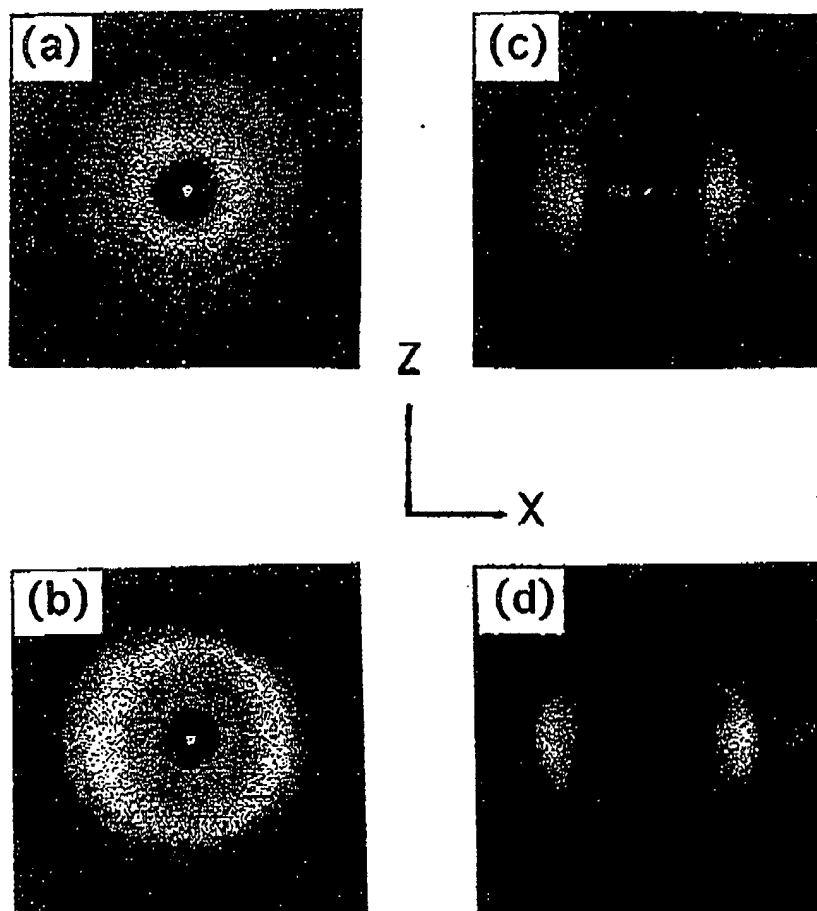


Fig. 2. X-Ray diagrams of PPTA film (Y pattern); (a) never-dried film; (b) film (Sample 2) dried at room temperature without dimensional restrictions; (c) film (Sample 3) dried at room temperature with constant dimensions; (d) film (Sample 1) produced by our procedure.

面配向、II型結晶は(010)面配向であった。高柳らは、水凝固によって生じたII型結晶からI型結晶への相転移は、製膜の際のポリマー原液の濃度が影響し、高濃度(15 wt%)ではほとんど起こらないと報告している³⁾。試料1のポリマー濃度は12 wt%で、高柳らが示した相転移可能な濃度範囲の上限に近いが、350℃以上の高温の定長乾燥では後述するようにII型結晶がI型結晶へ相転移した。これよりII型結晶からI型への結晶転移にはポリマー濃度だけでなく、乾燥条件も重要な因子となっているものと考えられる。

3.2 定長室温乾燥過程の構造変化

試料1フィルムの高度の面配向構造は製膜過程のどの段階で生じるのかを検討した^{7,9)}。試料1フィルムと同様の方法で製膜し、乾燥する直前の状態で取り出し、試料とした。このような未乾燥湿潤状態のフィルムではX線の入射方向に関係なく、どの反射もブロードなリング状となった(Fig. 2(a))。これはPPTAフィルムが未乾燥

状態では結晶性が非常に低く、結晶の配向がないことを示している。これより試料1フィルムの高度の配向構造はフィルムの乾燥過程で生じたことが明らかである。また、未乾燥湿潤状態フィルムのX線図には(200)、(004)、(006)面の反射はみえるが(010)面に相当する反射は認められず、この段階ではII型結晶形は現れなかった。

水凝固後、枠に固定せず自由端で室温乾燥した試料2フィルムのX線回折写真(Fig. 2(b))は、未乾燥フィルムに比べ各反射とも強度が増大した。しかし、どの反射もX線の入射方向に無関係に完全にリング状であり、無配向のままに結晶化が進んでいることがわかる。一方、枠に固定し定長で室温乾燥した試料3フィルムのX線回折写真(Fig. 2(c))では、各反射がシャープになった上、面配向構造がみられた。回折プロファイル(Fig. 4の1. Hold)には(200)面配向した微量のI型結晶の混在が認められるが、大きなII型結晶の(010)面のピークがみられた。これより試料3フィルムの基本構造は高柳らが

宮下・中尾・藤田・藤原・天野

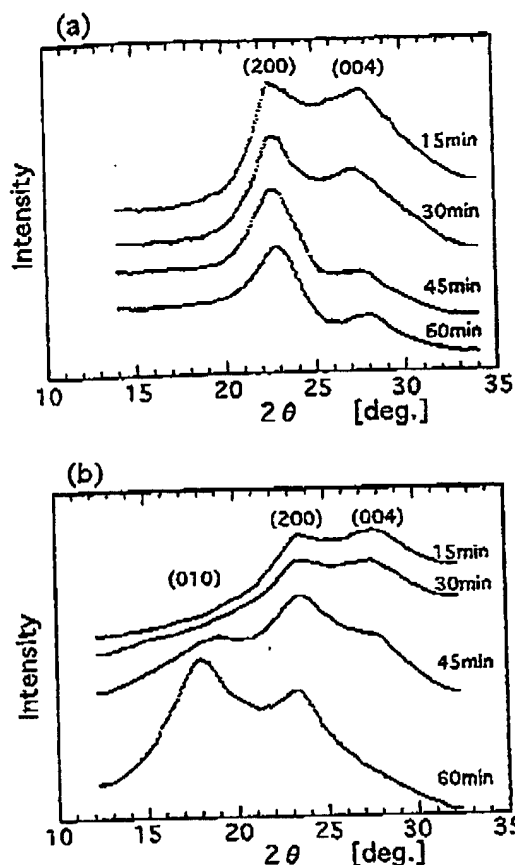


Fig. 3. Change in X-ray diffractograms of the PPTA film dried at room temperature with constant dimensions: (a) Y pattern; (b) X pattern.

見いだしたII型結晶の(010)面配向構造であるといえる。

未乾燥湿潤状態のフィルムを枠に固定し、室温で乾燥する過程の回折プロファイルの変化を追跡した。Fig. 3(a)はXパターン、Fig. 3(b)はYパターンである。Xパターンでは時間経過とともに(200)面の反射がシャープになり(004)面の反射が消失した。Yパターンでは(010)面の反射が際立って強くなった。Xパターンの(200)面の反射は(010)面配向したII型結晶によるものであり、Yパターンの(200)面の反射はI型結晶の(200)面配向によるものである。又、Yパターンの変化を総合すると、乾燥に伴ってII型結晶の結晶化と同時に配向構造が形成されていることがわかる。試料3フィルムの(010)面の反射強度は、試料2フィルムの(010)面の反射強度の比はるかに強く、同じ室温乾燥でも定長と自由端では、結晶形の発現の仕方に大きな差を生じた(Fig. 4)。II型結晶の発生は(010)面配向構造の形成と並行して進行しており、乾燥時に試料にかかる力が密接

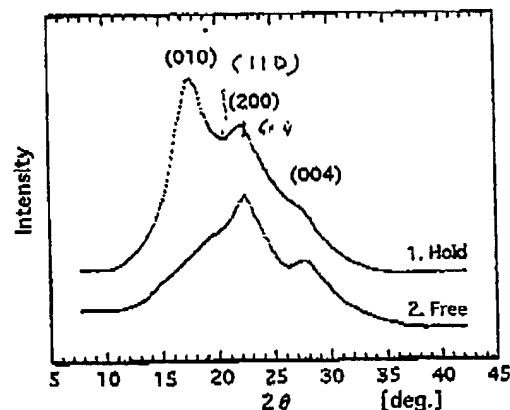


Fig. 4. X-ray diffractograms (Y pattern) of the film dried at room temperature under different drying conditions: 1, with constant dimensions (Hold); 2, without dimensional restrictions (Free).

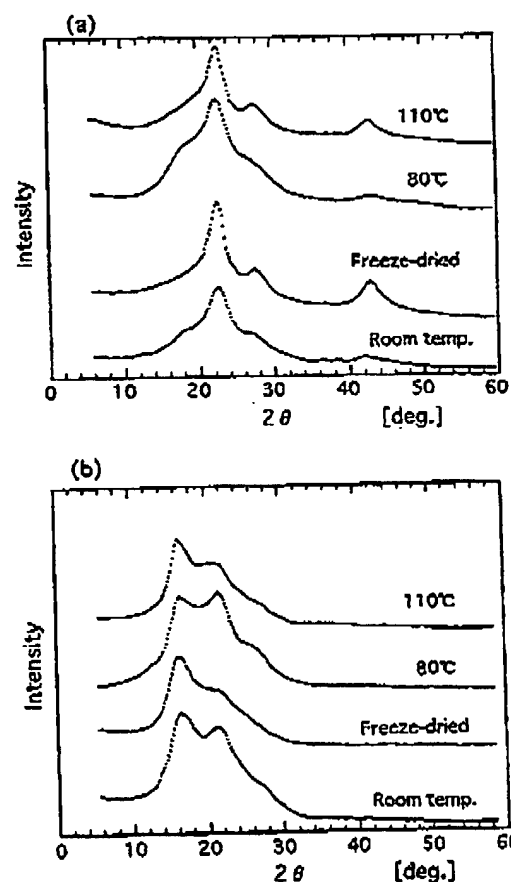


Fig. 5. X-Ray diffractograms of the film dried with constant dimensions under various drying conditions. X-Ray diffractograms were obtained (a) by the transmission method, and (b) reflection method.

芳香族ポリアミドフィルムの構造解析

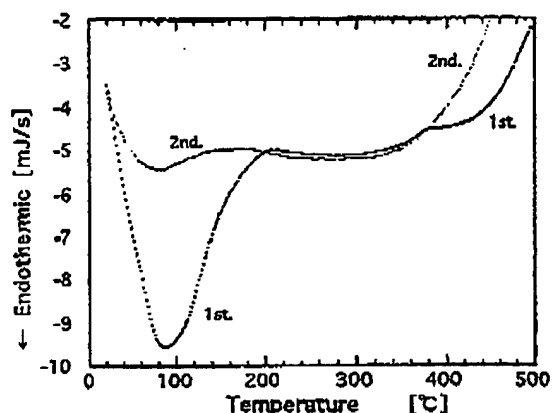


Fig. 6. DSC thermograms of the PPTA film dried with constant dimensions at room temperature: 1, 1st scan; 2, 2nd scan of the same sample.

に關係することを示唆している。

いろいろな条件で定長乾燥した試料の回折プロファイルを Fig. 5 に示す。透過法で得たパターン (Fig. 5(a)) と反射法で得たパターン (Fig. 5(b)) を比較するとフィルムの配向状態の特徴を知ることができる。定長室温乾燥の場合には、(010) 面の反射が透過法パターンより反射法パターンで強く、(010) 面がフィルム面に平行に選択的な配向をしていることがわかる。これは II 型結晶が (010) 配向していることを示す。これらのパターンを比較すると生成している結晶形はいずれも II 型であるが、フィルムからの急速な水の離脱を伴うような乾燥を経た試料ほど明確な配向構造がみられた。特に、凍結乾燥した試料では透過法パターンに (010) 面の反射がみられず、110°C の定長乾燥試料と同様に (010) 面配向構造となっていた。試料中の水を凍結させて乾燥することは、試料を 110°C で定長乾燥するのと同じ効果があることを示している。他の試料では透過法パターンにも (010) 面の反射が現れており配向に乱れがある。配向が乱れる傾向は、水の離脱のゆるやかな条件ほど著しくなっていた。

3.3 熱処理過程の構造変化

Fig. 6 に示した定長室温乾燥した試料 3 フィルムの DSC 曲線には、最初の昇温過程 (1st) で 100°C 付近を中心にフィルムに残存する水の蒸発による大きな吸熱ピークが現れた。さらに 320°C から 380°C にかけて階段状の変化があり、試料の比熱の変化が急激に変化したことを示している。一方、昇温した試料を一度室温まで下げ、再び昇温した DSC 曲線 (2nd) には、水の蒸発による吸熱ピークも、階段状変化もみられない。最初の昇温過程で DSC 曲線が階段状に変化する前後の温度 (270°C と 435°C) で DSC 装置から取り出した試料の X 線写真によると、フィルムの配向は良くなってきたが、II 型から

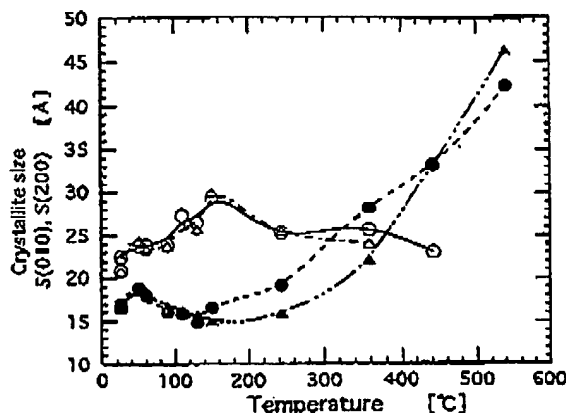


Fig. 7. Relation between the crystallite size and annealing temperature of the annealed film dried at room temperature with constant dimensions. Annealing was achieved with constant dimensions (○, ●), without dimensional restrictions (△, ▲), crystallite size (010) plane of mod. II (○, △), crystallite size (200) plane of mod. I (●, ▲).

I 型結晶への結晶転移は完了していなかった。しかし、フィルムの熱処理実験によると、この温度域は結晶転移と結晶化が最も顕著に進行する領域であり、DSC 曲線の階段状変化は PPTA 結晶の II 型から I 型結晶への結晶転移と I 型への結晶化に対応するものと考えられる。

自由端室温乾燥した無配向フィルム (試料 2) の熱処理 (120°C および 344°C で 2 分間) では、熱処理が定長か自由端であるのかの差はみられずフィルムは無配向のままであった。もともと微弱な (010) 面の反射強度はわずかに変化しても (200) 面の反射にはほとんど変化がなかった。これらのことから、試料 2 の無配向フィルムを定長で熱処理しても配向構造は生じないことがわかる。PPTA フィルムを無配向状態から配向させるためには、多量の水分子の脱離を伴う未乾燥湿潤状態からの乾燥過程でなければならない。

Fig. 7 は、定長室温乾燥フィルム (試料 3) を定長および自由端熱処理したフィルムの微結晶サイズ $S(200)$, $S(010)$ である。Fig. 7 より、熱処理温度が室温～約 200°C の範囲では微結晶サイズは定長、自由端によらず II 型結晶の $S(010)$ は増大するが、I 型結晶の $S(200)$ は減少した。逆に、熱処理温度が 250°C 以上になると $S(200)$ は定長、自由端ともに大きく増大し、 $S(010)$ はわずかに減少した。このように定長室温乾燥フィルムでは熱処理時の束縛条件によらず、水の蒸発温度領域では II 型結晶の (010) 面の成長が優先し、さらに高い温度領域では I 型結晶の (200) 面が成長すると考えられる。

また、Fig. 8(a) に I 型および II 型の結晶分率 $R(1)$, $R(2)$ を、Fig. 8(b) に結晶化度 X_c を示す。さらに、配向の目安 $H(010)$, $H(200)$ の変化を Fig. 9 に示す。Fig. 8 よ

宮下・中尾・藤田・藤原・天野

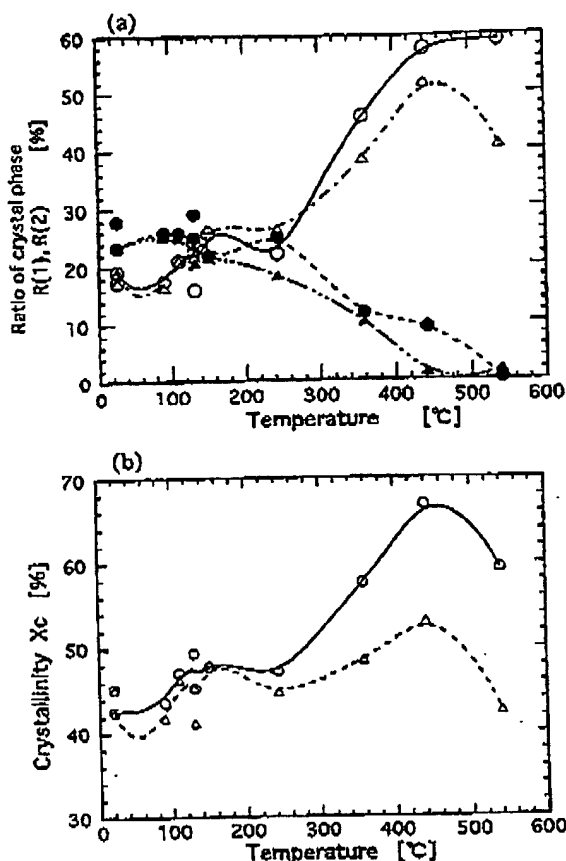


Fig. 8. Relation between the ratio of crystal modifications or crystallinity, and annealing temperature of the annealed film dried at room temperature with constant dimensions; (a) ratio of mod. I ($R(1)$) and mod. II ($R(2)$); (b) crystallinity X_c . Annealing was achieved with constant dimensions (O, ●), or without dimensional restrictions (Δ, ▲), $R(1)$: (O, Δ); $R(2)$: (●, ▲).

り、熱処理温度が室温～約 200°C の範囲で結晶化度 X_c と、I型およびII型のそれぞれの結晶分率 $R(1)$, $R(2)$ とは、定長、自由端によらず増大した。熱処理温度が 250°C 以上になると、 X_c と $R(1)$ は増大し、 $R(2)$ が急激に減少した。これは、熱処理によって非晶部が結晶化するとともに、水の蒸発温度領域ではII型結晶の成長が、そして水の蒸発温度を越えた高温領域ではII型からI型への結晶転移が進んだためと考えた。

なお、相転移の挙動には定長、自由端熱処理の違いは見られないが、熱処理条件による X_c の差から高温領域での結晶化は定長熱処理の方が起こりやすいといえる。さらに Fig. 9 によれば、(010) 面の配向の目安 $H(010)$ は処理温度に関係なくほぼ一定であった。これに対しI型結晶の(200)面の配向の目安 $H(200)$ は室温～約

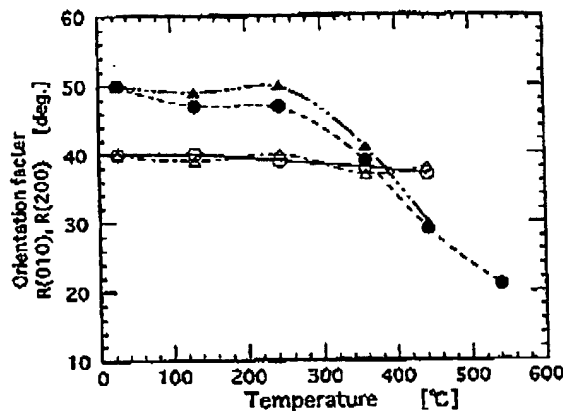


Fig. 9. Relation between the orientation factor $H(hkl)$ and annealing temperature of the annealed film dried at room temperature with constant dimensions. Annealing was achieved with constant dimensions (O, ●), or without dimensional restrictions (Δ, ▲), $H(010)$: (O, Δ); $H(200)$: (●, ▲).

200°C では変らず、250°C 以上では急激に減少し、配向が良くなった。水の蒸発温度領域では、 $H(200)$ は定長熱処理の方が自由端熱処理に比べて小さいが高温領域ではその差は縮まった。

4 ま と め

高柳らの報告ではフィルム製膜時の束縛条件については触れていなかった。しかし、製膜時の束縛条件はフィルムの配向構造を決定する重要な因子となっている。我々の結果をまとめると、

(1) 凝固直後の未乾燥フィルムは結晶性は低く、無配向であり、II型結晶も認められない。フィルムの配向構造は未乾燥状態からの乾燥過程でII型結晶の生成とともに形成される。

(2) 自由端室温乾燥フィルムは、無配向で、かつII型結晶がわずかに存在する。これに対し、定長室温乾燥フィルムは(010)面配向しており大部分がII型結晶である。これは、水の蒸発過程で外力が働くと水素結合面が優先的にフィルム面に垂直になるよう配向し、II型結晶が成長するためと考えた。従って、水の蒸発と同時に定長条件が満たされることが、II型の結晶発生の重要な要件であると考えられる。

(3) 定長室温乾燥フィルムを熱処理すると、フィルム中の水が蒸発する温度領域では(010)面配向したII型結晶が優先的に成長する。これは、未乾燥フィルムの定長乾燥過程でII型結晶の(010)面配向構造が形成することに対応していると考えた。高温域では束縛条件に関係なく、(010)面配向したII型結晶が(200)面配向したI型結晶に転移する。これは、PPTAフィルムではI型結

芳香族ポリアミドフィルムの構造解析

晶の(200)面配向の方がII型結晶の(010)面配向構造よりも、エネルギー的に安定であることを意味していると考えた。水素結合面がフィルム面に対して垂直に立っているII型結晶の(010)面配向は、高柳らの指摘するように系中の水分子を蒸発させるのに適した構造であると考えられる。水の蒸発過程で配向を固定できるような条件下では、エネルギー的には不利なII型結晶も成長することができると考えられる。

(4) 定長室温乾燥フィルムは熱処理によって、結晶化とともにII型からI型へ結晶転移する。配向構造の変化を伴うこの結晶転移では、(200)面および(010)面の配向性が一次的にも悪くなることはない。また、結晶転移と配向変化は同時に生じている点の特徴である。このような転移は水素結合面間のスリップ、分子鎖軸周りの回転による水素結合方向の転移など比較的小さい範囲の運動によるものであると考えられる。

謝 辞 本報文の内容は第38回高分子討論会(1989年福井大学)、第39回高分子討論会(1990年、名古屋大学)において発表した。試料作成など御援助いただいた旭化成工業(株)MKFプロジェクトの方々に感謝します。

文 献

- 1) J. E. Flood, J. L. White, and J. P. Feller, *J. Appl. Polym. Sci.*, **27**, 2965 (1982).
- 2) K. Haraguchi, T. Kajiyama, and M. Takayanagi, *J. Appl. Polym. Sci.*, **23**, 903 (1979).
- 3) K. Haraguchi, T. Kajiyama, and M. Takayanagi, *J. Appl. Polym. Sci.*, **23**, 915 (1979).
- 4) K. Tashiro, K. Kobayashi, and H. Tadokoro, *Macromolecules*, **10**, 413 (1977).
- 5) T. Amano, T. Fujita, T. Fujiwara, E. Sato, and K. Nagasawa, *Polym. Eng. Sci.*, **29**, 1237 (1989).
- 6) 笠谷秀雄, 藤田忠宏, 藤原 隆, 長沢啓作, 村岡望光, 天野敬彦, *繊維学会誌*, **48**, 1 (1992).
- 7) N. Miyashita, T. Amano, H. Yamauchi, T. Fujita, and T. Fujiwara, *Polym. Prepr. Jpn.*, **38**, 3344 (1989).
- 8) T. Nakao, T. Amano, T. Fujita, and T. Fujiwara, *Polym. Prepr. Jpn.*, **38**, 1105 (1990).
- 9) T. Amano, T. Nakao, N. Miyashita, T. Fujita, and T. Fujiwara, *Reprint, the 6th Annual Meeting, Polymer Processing Society (PPS), Nice (1990)*.

Structural Analysis of Poly(*p*-phenylene terephthalamide) Films from Liquid Crystalline Solutions

Norikazu MIYASHITA^{*1}, Tatsuya NAKAO^{*1}, Tadahiyo FUJITA^{*2}, Takashi FUJIWARA^{*2}, and Toshihiko AMANO^{*3}

^{*1} Analytical Research Center, Asahi Chemical Industry (5-4960, Nakagawara, Nobeoka, Miyazaki, 882 Japan)

^{*2} MKF Project, Asahi Chemical Industry (5-4960, Nakagawara, Nobeoka, Miyazaki, 882 Japan)

^{*3} Faculty of Home Economics, Mukogawa Women's University (6-46, Ikebāraki, Nishinomiyā, Hyogo, 663 Japan)

Poly(*p*-phenylene terephthalamide) (PPTA) films were formed from a liquid crystalline sulphuric acid solution using water as a coagulant. The polymer dope with optical anisotropy was cast on a flat plate. The phase transition from the optical anisotropy to isotropy was accomplished by means of controlling temperature and humidity, and then the cast dope was immersed in a coagulation bath. When the film was dried at room temperature after the coagulation without any dimensional restrictions, crystallites in the film were randomly oriented. The (010) reflection of the type II modification of the PPTA crystal was hardly found in the X-ray diagram of the film. When the drying at room temperature was carried out with constant dimensions, the film showed the (0*h*0) planar orientation of the type II crystal. If the film was annealed at higher temperatures, the II crystal was transformed to the type I crystal and the film orientation changed at the same time towards the (*h*00) planar orientation. A never-dried film exhibited very low crystallinity and random orientation. The drying process with dimensional restrictions proves to be an important factor in both generating the type II crystal and forming the planar orientation.

KEY WORDS Poly(*p*-phenylene terephthalamide) Films / Crystal Structure / Phase Transition /

X-Ray Diffraction / Planar Orientation /

(Received March 28, 1994; Accepted May 11, 1994)

[*Kobunshi Ronbunshu*, **51**(11), 745—751 (1994)]

Characterization of Magnetic Tapes and Substrates

Brian L. Weick and Bharat Bhushan, *Senior Member, IEEE*

Abstract—Ultra-thin advanced magnetic tape substrates are shown to have superior characteristics when compared to PET. In particular, PEN and ARAMID are viable alternatives to PET with elastic moduli that range from 4–5.4 GPa for PEN, and 10 GPa for ARAMID. Also, the ARAMID material is more isotropic than PET or PEN with a higher glass transition temperature of 277°C. Thermal and hygroscopic expansion measurements show that PEN and ARAMID are typically superior to PET. Characteristics of two developmental materials (a polybenzoxazole and a polyimide) are also presented.

I. INTRODUCTION

ALTERNATIVE polymeric materials are currently being studied to replace poly(ethylene terephthalate) or PET as the substrate for magnetic tapes. Current data base grade PET is typically 14.4 μm thick, and the ultra-thin alternative substrates include poly(ethylene naphthalate) or PEN which is 4.5 μm thick, an aromatic polyamide (ARAMID) which is 4.4 μm thick, a polyimide (PI) which is 7.6 μm thick, and poly(benzoxazole) or PBO which is 5.0 μm thick. Such thinner substrates allow for a higher volumetric density when a magnetic tape is wound onto a reel. For example, to make an advanced storage device with a volumetric density of one terabyte per cubic inch the following characteristics are required: a substrate which is approximately 4 μm thick, a magnetic medium with a track density of about 9000 tracks per inch with a 64 head array and 8 head positions, and a linear density of about 160 kbits/inch. To make a magnetic tape with such high areal densities the substrate must be mechanically and environmentally stable with a high surface smoothness. For high track densities, lateral contraction of the substrates from thermal, hygroscopic, viscoelastic, and/or shrinkage effects must be minimal. To minimize stretching and damage during manufacturing and use of thin magnetic tapes, the substrate should be a high modulus, high strength material with low viscoelastic and shrinkage characteristics. If the storage device is a linear tape drive, any linear deformations can be accounted for by a change in clocking speed [1]. However, if the storage device is a rotary tape drive, anisotropic deformations of the substrate would be undesirable. To minimize stretching during use of thinner substrates, the modulus of elasticity, yield strength, and tensile strength should be

high along the machine direction. Also, since high coercivity magnetic films on metal evaporated tapes are deposited and heat treated at elevated temperatures, a substrate with stable mechanical properties up to a temperature of 100–150°C or even higher is desirable. Since magnetic recording devices require low motor torque and high magnetic reliability, the finished magnetic medium must also exhibit low friction/stiction and high durability. In addition to mechanical and environmental stability, the cost of the material is also a major factor in the selection of a suitable substitute for PET. Lastly, various long-term reliability problems including uneven tape-stack profiles (or hardbands), mechanical print-through, instantaneous speed variations, and tape stagger problems can all be related to the substrate's viscoelastic characteristics [1].

Perette *et al.* [2], [3], have presented some material property information about advanced tape substrates including tensile properties as well as expansion and shrinkage characteristics. Although extensive characterization research has been performed on PET [1], such research on alternative polymeric films is not readily available.

The objective of this research was to measure mechanical, hygroscopic, thermal, viscoelastic, and shrinkage characteristics of alternative substrates for flexible magnetic media. In addition, these characteristics were measured for magnetic tapes which use ultra-thin PET film. A detailed description of the substrates and tapes can be found in [4].

II. EXPERIMENTAL

Mechanical property measurements were made using a Monsanto Tensometer T20 tensile test machine in accordance with ASTM Spec. 1708. Thermal expansion measurements (CTE) were made in accordance with ASTM D696-79 using a Zygo Laser Dimension Sensor. Specimens cut into $13 \times \frac{1}{2}$ in. strips were used for CTE, and the temperature was varied from 24–46°C. Hygroscopic expansion measurements (CHE) were made using a Neenah Paper Expansimeter. The humidity was varied from 27–95% using a salt solution, and $5 \times \frac{1}{2}$ inch specimens were used. Glass transition temperatures were measured using a Rheometrics RSA-II Dynamic Mechanical Thermal Analyzer (DMTA). Viscoelastic and shrinkage characteristics were measured using techniques described in [4], [5]. Where applicable, all the characterization measurements were made for both the machine (MD) and transverse (TD) directions. (Measurements for PET were made along the major (MAJ) and minor (MIN) optical

Manuscript received June 9, 1995; revised December 11, 1995. This research was sponsored by the National Storage Industry Consortium/Advanced Research Projects Agency (Grant MDA 972-93-1-0009).

The authors are with the Computer Microtribology and Contamination Laboratory, Department of Mechanical Engineering, The Ohio State University, Columbus, OH 43210, U.S.A.

Publisher Item Identifier: S 0018-9464(96)03075-0.

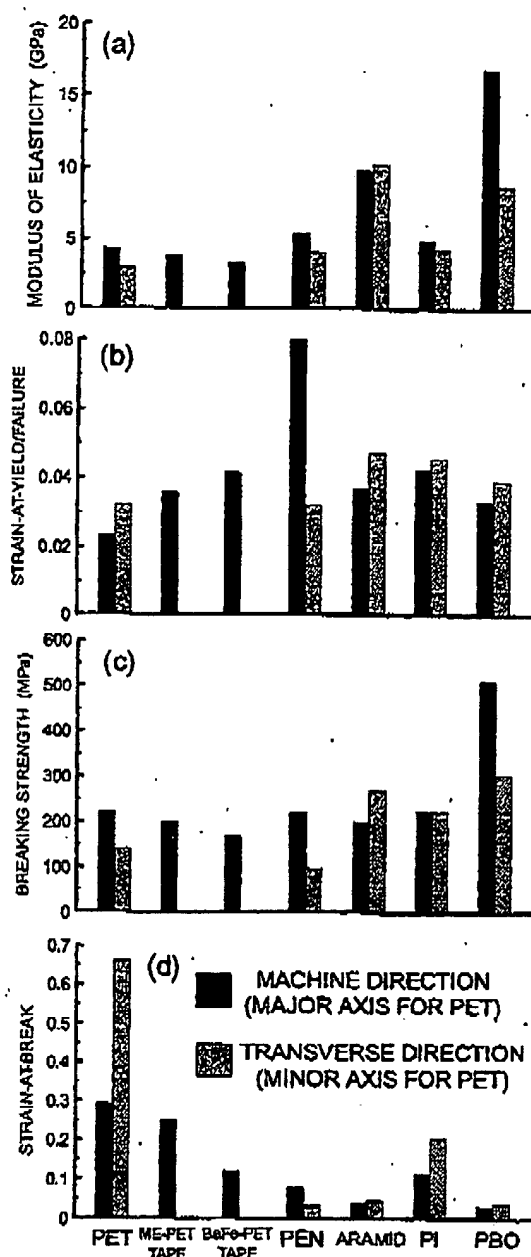


Fig. 1. Mechanical Properties of Magnetic Tape Substrates.

axes which show the extinction of light when viewed under a cross-polarizer.)

III. RESULTS AND DISCUSSION

A. Mechanical Properties

Mechanical properties of the tapes and substrates are presented in Fig. 1. Properties measured include modulus of elasticity, strain-at-yield/failure, breaking strength, and strain-at-break. The strain-at-break measurements correspond with the strain at which the substrates break, and the strain-at-yield/failure measurements correspond with

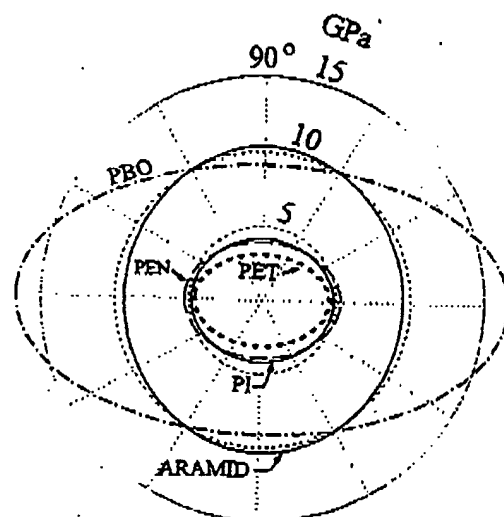


Fig. 2. Anisotropy in Modulus of Elasticity for Magnetic Tape. Substrate: 0°: Machine Direction (Major Axis for PET); 90°: Transverse Direction (Minor Axis for PET).

the strain at which the substrates start to deform irreversibly. Figure 1a shows modulus of elasticity measurements for PET, two PET tapes, and the alternative substrates. PEN, ARAMID, PI, and PBO all offer improvements in elasticity when compared to 3-4 GPa for PET. Elastic moduli range from 4-5.4 GPa for PEN, 5-6 GPa for ARAMID, 4-5 GPa for PI, and 9-17 GPa for PBO. The alternative substrates also offer improvements in breaking strength when compared to PET and PET tapes. Therefore, based on a typical tape tension of 7 MPa (1000 psi), the alternative materials would be stressed to only a fraction of their breaking strength (typically $\frac{1}{10}$ to $\frac{1}{30}$). Strain-at-break measurements indicate that PET tends to be more ductile than the alternative substrates. However, for PET irreversible strain occurs at the yield point. This is indicated in Fig. 1b, and strains of only 0.02 to 0.03 were measured when PET begins to yield. The PET tapes yield at slightly higher strains of 0.03 to 0.04. PI also fails at its yield point, but PEN, ARAMID, and PBO do not have yield points. Instead they fail irreversibly only at their breaking points. The failure strains for the alternative substrates are typically higher than those measured for PET ranging from 0.03 to 0.08 for PEN, 0.035-0.05 for ARAMID, 0.04-0.045 for PI, and from 0.03 to 0.04 for PBO.

Anisotropic characteristics of the tape substrate materials are shown in Fig. 2. Modulus of elasticity measurements along different material orientations are shown in this polar plot. Since ARAMID has a circular curve, it is a relatively isotropic material with an elastic modulus of approx. 10 GPa regardless of material orientation. PI is also relatively isotropic, but its modulus is significantly less than ARAMID's. PET and PEN not only have low moduli, but they are anisotropic materials as indicated by their elliptical curves. Fig. 2 also shows that even though PBO has a high modulus, it is also anisotropic.

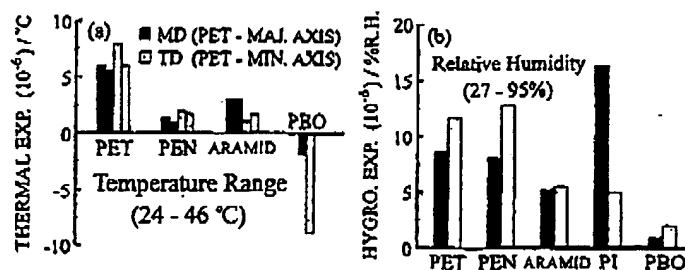


Fig. 3. Thermal and hygroscopic expansion measurements.

TABLE I
SUMMARY OF MECHANICAL, HYGROSCOPIC, THERMAL, VISCOELASTIC, AND SHRINKAGE CHARACTERISTICS OF MAGNETIC TAPE SUBSTRATES

Material	Mod. of Elasticity (GPa)	Strain at Yield/Failure	Breaking Strength (MPa)	Strain at Break	Density g/cm ³	Moist. Absorb. (%)	CHE (27-95%) (10 ⁻⁶)/%RH	CTE (24-46 °C) (10 ⁻⁶)/°C	T _g (°C)	Melting Point (°C)	Creep-Compl. 100 hrs @ 50 °C (GPa ⁻¹)	Lat. Contract. 100 hrs @ 50 °C (μm)	Shrinkage 100 hrs @ 50 °C (%)
PET	MAJ	4.3	0.02	221	0.28	1.395	0.4	8.5	6.0	116	0.35	9.3	neg.
	MIN	2.9	0.03	141	0.68			11.7	7.9		0.47	12.5	
PEN	MD	5.4	0.08	222	0.08	1.355	0.4	8.1	1.5	158	0.23	6.1	0.034
	TD	4.1	0.03	298	0.03			12.9	1.9		0.36	9.8	0.034
ARAMID	MD	9.8	0.04	200	0.04	1.500	1.5	5.3	3.1	277	0.18	4.8	0.011
	TD	10.2	0.05	271	0.05			5.5	1.0		0.18	4.3	neg.
PI	MD	4.8	0.04	227	0.12	1.420	2.9	13.0	—	360-410	0.33	8.6	neg.
	TD	4.2	0.05	223	0.21			—	—		0.27	7.1	neg.
PBO	MD	16.8	0.03	511	0.03	1.540	0.8	1.0	-2.0	—	0.069	1.84	neg.
	TD	8.8	0.04	305	0.04			2.0	-8.0		0.067	1.79	neg.

References [1], [9].

*24 hrs @ 22 °C.

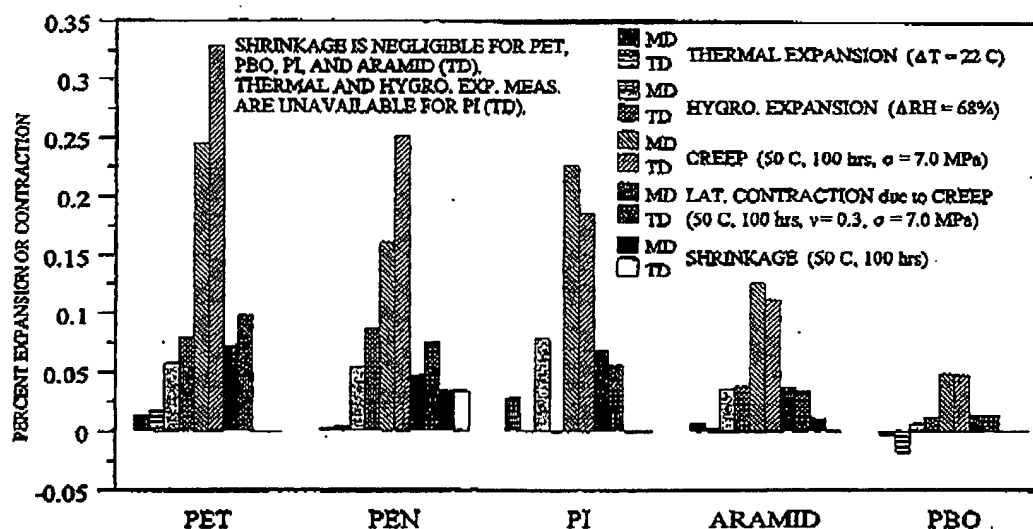
*Calculated from creep-compliance data for a 12.7 mm wide substrate using a Poisson's ratio of 0.3 and $\sigma=7.0$ MPa.

Fig. 4. Summary of expansion and contraction characteristics where the data has been reduced to a percentage scale.

B. Thermal and Hygroscopic Properties

CTE and CHE measurements are presented in Figs. 3a and b. ARAMID and PEN have lower thermal expansion characteristics than PET. However, only ARAMID and PBO show a significant decrease in hygroscopic expansion. The glass transition temperature (T_g) for ARAMID was measured to be 277 $^{\circ}\text{C}$ versus 156 $^{\circ}\text{C}$ for PEN and 116 $^{\circ}\text{C}$ for PET. A T_g could not be measured for PBO, and polyimides have T_g 's ranging from 360-410 $^{\circ}\text{C}$ [1].

IV. SUMMARY AND CONCLUSIONS

A summary of the characteristics measured for magnetic tape substrates is presented in Table I, and CTE, CHE, creep, lateral contraction, and shrinkage measurements are presented on a percentage basis in Fig. 4. Although it has the best characteristics, PBO will be ruled out as an alternative to PET due to its current lack of availability. PI offers only a slight improvement over PET, and availability of PI is also a concern. ARAMID

and PEN both offer improved expansion and contraction characteristics when compared to PET. Although these materials shrink slightly more than PET at 50°C, their expansion and contraction characteristics are lower. (The shrinkage for PEN and polyesters in general could be reduced by stress-stabilizing the material at 65°C [1], [5].) ARAMID and PEN are also closer to the contraction criteria for an advanced magnetic tape with 256 tracks per inch to be read at a time. Based on this criteria lateral contraction should be less than 0.08% if a $\frac{1}{16}$ track mismatch is tolerable and the head can be recentered. A clear choice between ARAMID and PEN cannot be made although ARAMID has a higher T_g than the polyester films which makes it more suitable for metal evaporated tapes. Also, the elastic modulus is a factor of two higher for ARAMID when compared to PEN, and ARAMID is more isotropic which renders it more compatible with rotary tape drives. However, PEN has a creep velocity which is lower than that for ARAMID, and the creep velocity for PEN continues to decrease after 100 hours at 50°C. In comparison, ARAMID continues to deform viscoelastically at the same rate [4]. The final choices for alternative substrates can be ranked as follows: first choice - PBO (unavailable), second choice - PEN or ARAMID, third choice - PI (availability in question), fourth choice - PET.

IV: ACKNOWLEDGMENT

We would like to thank Don Gustafson at NML/3M for performing the thermal, hygroscopic, and T_g measurements, and Reuben Mees for his assistance with mechanical measurements.

REFERENCES

- [1] B. Bhushan, *Mechanics and Reliability of Flexible Magnetic Media*. New York: Springer-Verlag, 1992, pp. 85-437.
- [2] D. Peretti, W. Hwang, P. Pierini, D. Spiliotis, J. Judy, and Q. Chen, "A high-performance, flexible substrate for thin-film media," *J. of Mag. and Mag. Mater.*, vol. 120, pp. 334-337, 1993.
- [3] D. Peretti and P. Pierini, "Advanced substrates for high performance flexible media," in *Advances in Magnetic Recording*, ed. D. Spiliotis, Amsterdam: Elsevier in press.
- [4] B. L. Weick and B. Bhushan, "Shrinkage and viscoelastic behavior of alternative substrates for magnetic tapes," *IEEE Trans. on Mag.*, vol. 31, pp. 2937-2939, 1995.
- [5] B. L. Weick and B. Bhushan, "Viscoelastic and shrinkage behavior of ultra-thin polymeric films," *J. Appl. Polym. Sci.*, vol. 58, pp. 2381-2398, 1995.

Bharat Bhushan, received the MS in mechanical engineering from the Massachusetts Institute of Technology, the MS in mechanics and the Ph.D. in mechanical engineering from the University of Colorado at Boulder; MBA from Rensselaer Polytechnic Institute at Troy, NY; and an D.Sc. (Tech.) from the University of Trondheim at Trondheim, Norway.

He has worked for the Department of Mechanical Engineering at the Massachusetts Institute of Technology, Cambridge, MA; Automotive Specialists, Denver, CO; the R&D Division of Mechanical Technology Inc., Latham, NY; the Technology Services Division of SKF Industries Inc., King of Prussia, PA; the General Products Division Laboratory of IBM Corporation, Tucson, AZ; the Almaden Research Center of IBM Corporation, San Jose, CA; and the Department of Mechanical Engineering at the University of California, Berkeley, CA. He is presently an Ohio Eminent Scholar Professor in the Department of Mechanical Engineering and the Director of Computer Microtribology and Contamination Laboratory at the Ohio State University, Columbus, Ohio.

Dr. Bhushan has authored three technical books, 12 handbook chapters, more than 250 technical papers in refereed journals, and more than 60 technical reports. He has edited more than 13 books, and holds five US patents. He is editor-in-chief of *World Scientific Advances in Information Storage Systems*, Series and CRC Press *Mechanics and Materials Science Series*. He has received more than a dozen awards for his contributions to science and technology from professional societies, industry, and U.S. government agencies. He is a fellow of ASME and the New York Academy of Sciences, a senior member of IEEE, and the member of STLE, NSPE, Sigma Xi and Tau Beta Pi.

Ab
tions
read
sions
trial
and
pole
a sin
vary
exam
shift
netiz
in co
head
singl
most
pole.

T
read
cord
mun
and
to
loda
topu
Si
for
tunc
publ
stan
ence
and
und
have
to
M
H
Statis
Univ
D
thical
Tech
1994
Pi

**This Page is Inserted by IFW Indexing and Scanning
Operations and is not part of the Official Record**

BEST AVAILABLE IMAGES

Defective images within this document are accurate representations of the original documents submitted by the applicant.

Defects in the images include but are not limited to the items checked:

- ☐ **BLACK BORDERS**
- ☐ **IMAGE CUT OFF AT TOP, BOTTOM OR SIDES**
- ☐ **FADED TEXT OR DRAWING**
- ☐ **BLURRED OR ILLEGIBLE TEXT OR DRAWING**
- ☐ **SKEWED/SLANTED IMAGES**
- ☐ **COLOR OR BLACK AND WHITE PHOTOGRAPHS**
- ☐ **GRAY SCALE DOCUMENTS**
- ☐ **LINES OR MARKS ON ORIGINAL DOCUMENT**
- ☒ **REFERENCE(S) OR EXHIBIT(S) SUBMITTED ARE POOR QUALITY**
- ☐ **OTHER: _____**

IMAGES ARE BEST AVAILABLE COPY.

As rescanning these documents will not correct the image problems checked, please do not report these problems to the IFW Image Problem Mailbox.